37, 155. J. Phys. Chem. 1963, 67, 853.
(38) Dexter, D. L. J. Chem. Phys. 1973, 21, 836.
(39) Dose, E. V.; Hoselton, M. A.; Sutin, N.; Tweedle, M. F.; Wilson, L. J. J. Am. Chem. Soc. 1978, 100, 1141.
(40) The Stokes shifts of the emission from the MLCT states of $Ru(bpy)_3^{2+}$ and $Os(bpy)_3^{2+}$ are relatively small: see ref 28.
(41) Konig, E.; Watson, K. J. Chem. Phys. Lett. 1970, 6, 457.
(42) A value of ~0.5 eV is calculated assuming that the Franck-Condon or distortion energy of the excited state is equal to $6f(\Delta a_0)^2/2$ where Δa_0 is the difference between the iron-nitrogen bond lengths in the ground and excited states (0.14 Å) and f is a breathing force constant. The value of f was taken as that of $Fe(H_2O)_6^{2+}$ (1.6×10^5 dyn cm^{-1}; see: Sutin, N. In "Tunneling in Biological Systems", Chance, B., DeVault, D. C., Frauenfelder, H., Marcus, R. A., Schrieffer, J. R., Sutin, N., Eds.; Academic Press: New York, 1979; p 201.
(43) Dwyer, F. P.; Gyarfas, E. C. J. Am. Chem. Soc. 1954, 76, 6320.
(44) The difference between iron-nitrogen distances in $Fe(phen)_3^{2+}$ and $Fe(phen)_3^{3+}$ is less than 0.01 Å (ref 45 and 46).
(45) Zalkin, A.; Templeton, D. H.; Ueki, T. Inorg. Chem. 1973, 12, 1641.
(46) Baker, J.; Engelardt, L. M.; Figgis, B. N.; White, A. H. J. Chem. Soc., Dalton Trans. 1975, 530.
(47) Calculated using 385 cm^{-1} for the iron-nitrogen stretching frequency of $Fe(bpy)_3^{3+}$. See: Saito, Y.; Takemoto, J.; Hutchinson, B.; Nakamoto, K. Inorg. Chem. 1972, 11, 2003.
(48) Observed rates are generally 10^3 times slower than calculated rates in systems of this type (see ref 15 and 28).
(49) Ohsawa, Y.; Saji, T.; Aoyagui, S. J. Electroanal. Chem., submitted for publication.

Influence of Crystal Packing on the $\eta^1 \rightarrow \eta^3$ Rearrangement of an Allyl Ligand. Solution and Solid-State Structures of the Tetraphenylborate and Hexafluorophosphate Salts of a Platinum Allyl Cation

Carolyn Pratt Brock* and Thomas G. Attig

Contribution from the Department of Chemistry, University of Kentucky, Lexington, Kentucky 40506. *Received May 29, 1979*

Abstract: In acetone or methanol solution the reaction of $\{trans\text{-}PtH(solvent)(PEt_3)_2\}^+$ with *trans*-dimethyl 1-methylenecyclopropane-2,3-dicarboxylate affords a single product which is shown by infrared and NMR spectroscopy to contain the $\{Pt[\eta^1\text{-}CH(COOCH_3)C(COOCH_3)=CHCH_3](PEt_3)_2\}^+$ cation. The crystal structure of its tetraphenylborate salt (space group C_{2v}^9-$Pna2_1$, a = 28.302 (5), b = 12.382 (2), c = 12.741 (2) Å) has been determined by conventional X-ray diffraction methods (2267 observations, 300 variables, final R index on F_o of 0.037) and shows the cation to have the η^1-allyl structure given above. In crystals of the hexafluorophosphate salt, however (space group C_{2h}^5-$P2_1/c$, a = 10.191 (2) Å, b = 13.348 (3) Å, c = 21.351 (5) Å, β = 100.02 (2)°, 8314 observations, 307 variables, R index on F_o of 0.034), the cation has the quite different structure $\{Pt[\eta^3\text{-}CH_3CHC(CO_2CH_3)CHCO_2CH_3](PEt_3)_2\}^+$. This $\eta^1 \rightarrow \eta^3$ allyl rearrangement, which in the solid state is dependent on the identity of a noncoordinating anion, is not observed in solution by either infrared or NMR spectroscopy. The change in the dominant form of the cation of the PF_6^- salt upon crystallization is an example of stabilization by crystal packing of a structure which is not important in other phases, and is strong evidence that the η^1 and η^3 structures are related by a low-energy pathway.

Allyl groups usually bond to Pt(II) as either η^1 (I) or η^3 (II) ligands. The effects of ancillary ligands and solvent on the

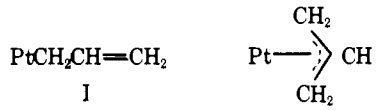

I II

mode of coordination have been described. Trialkylphosphines are more conducive to the formation of η^1 complexes than are triarylphosphines so that under the same reaction conditions oxidative addition of allyl halides to $Pt(PEt_3)_4$ and $Pt(PPh_3)_4$ leads to the isolation of *trans*-$Pt(\eta^1\text{-allyl})X(PEt_3)_2$ and $[Pt(\eta^3\text{-allyl})(PPh_3)_2]^+X^-$, respectively.[1,2] In the specific case of C_3H_5Cl and PPh_3 the neutral η^1 complex appears to be favored in benzene solution while the ionic η^3 form is dominant in chloroform.[3]

NMR studies also suggest that these two modes of coordination are similar energetically. Some η^3-allyl complexes of Pt(II) have been shown to undergo syn-anti exchange which can be slowed at low temperature, and a mechanism involving an η^1-allyl specie as an intermediate has been proposed.[2,4] The structure of a single crystal of *trans*-$Pt(\eta^1\text{-}C_3H_5)Cl(PPh_3)_2$ isolated from a bulk solution of the corresponding dynamic η^3 complex is evidence for such a process.[3] Kurosawa et al.[5] suggest that three intermediates are important in the exchange; a *cis*-η^1-allyl complex, a *trans*-η^1-allyl complex, and a neutral η^3-allyl complex formed by the dissociation of a phosphine followed by the coordination of the halide.

In studies of the cyclopropane ring-opening reaction of Feist's esters by Pt(II) hydrides[6,7] we have found that the product of the reaction is influenced not only by the coordi-

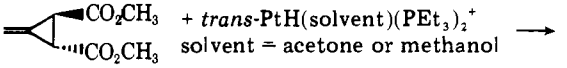

nating ability of the anion and, in solution, by the solvent, but is also influenced in the solid state by packing interactions. Herein we describe the solution and solid-state infrared spectra, NMR spectra, and crystal structures of two cationic Pt(II) allyl complexes which differ only in anion (BPh_4^- and PF_6^-). Although both salts have the η^1 structure in solution, the PF_6^- salt crystallizes as the η^3-allyl; the cation of the BPh_4^- salt is the expected η^1-allyl. To our knowledge this is the first crystallographic study of a system in which the bonding mode of a ligand depends on the identity of a noncoordinating counterion.

Counterion effects in the solid state have been observed previously for both cationic and anionic linkage isomers of SCN^- and $SeCN^-$.[8,9] For example, in the sterically hindered complex $Pd(Et_4dien)X^+$ (Et_4dien = 1,1,7,7-tetraethyldiethylenetriamine; X = SCN^-) the bonding mode of X is anion dependent. In the solid state the BPh_4^- salt is more stable as the S-bonded thiocyanate while the PF_6^- and SCN^- salts are

0002-7863/80/1502-1319$01.00/0

Table I. Summary of Crystal Data and Details of Intensity Collection and Refinement

compd	BPh_4^- salt	PF_6^- salt
formula	$C_{44}H_{61}BO_4P_2Pt$	$C_{20}H_{41}F_6O_4P_3Pt$
formula wt	921.8 amu	747.5 amu
space group	C_{2v}^9-$Pna2_1$	C_{2h}^5-$P2_1/c$
a	28.302 (5) Å	10.191 (2) Å
b	12.382 (2) Å	13.348 (3) Å
c	12.741 (2) Å	21.351 (5) Å
β		100.02 (2)°
vol	4464.9 Å^3	2860.1 Å^3
Z	4	4
density	1.371 g cm^{-3} (calcd) 1.37 (1) g cm^{-3} (obsd)	1.736 g cm^{-3} (calcd) 1.73 (1) g cm^{-3} (obsd)
crystal dimensions	0.08 × 0.22 × 0.31 mm	0.20 × 0.34 × 0.55 mm
bounding planes	{100}, {011}, (210), (2$\bar{1}$0)	{100}, {012}, ($\bar{1}$02)
temp	24 ± 1 °C	24 ± 1 °C
radiation	Mo Kα (graphite monochromator)	Mo Kα (graphite monochromator)
μ	32.70 cm^{-1}	51.65 cm^{-1}
transmission factors	0.494-0.773	0.201-0.392
take-off angle	2.0°	2.2°
scan rate	20°/min to 0.6°/min (θ)	20°/min to 1.0°/min (θ)
	depending on prescan (target signal-to-noise ratio 50:1)	
scan range	0.8° (2θ) below Kα_1 to 0.8° above Kα_2	1.0° (2θ) below Kα_1 to 1.0 above Kα_2
	extended by 25% on each side for background	
2θ limits	2-50°	2-60°
observations	$+h, +k, +l$ Friedel pairs for $2\theta \leq 10°$	$+h, +k, \pm l$
p factor	0.03	0.03
unique data	4108	8314
unique data with $F_o^2 \geq 3\sigma(F_o^2)$	2267 (ignoring Friedel pairs)	5651
final no. of variables	300	307
R on F ($\geq 3\sigma$)	3.7%	3.4%
R on F^2 (all data)	9.5%	7.6%
R_w on F ($\geq 3\sigma$)	3.9	4.0
error in observation of unit weight	1.50 electrons	1.63 electrons

more stable as the N-bonded isothiocyanates. These systems, however, have not been studied crystallographically, and, although the bonding modes of the ambidentate ligands have been rationalized as crystal packing effects, the presence of special interactions (other than those of the van der Waals type) has not been excluded.

Experimental Section

Crystal Structure of the BPh_4^- Salt. Crystals[7] were grown by slow evaporation of a CH_3OH/CH_2Cl_2 solution and were mounted in air. Data were collected with an Enraf-Nonius CAD-4/F diffractometer; details are summarized in Table I. Unit-cell data were determined as part of a least-squares fit of the setting angles of 25 reflections having $2\theta > 20°$. The symmetry and extinctions of the photographically observed diffraction pattern identify the crystal as belonging to either the centrosymmetric space group *Pnma* or the noncentrosymmetric group $Pna2_1$. The latter was indicated by the value of 4 for Z (the cation cannot accommodate imposed symmetry without substantial disorder), the Wilson statistics, and significant intensity differences between the Friedel pairs. This choice was confirmed by the three-dimensional Patterson function, which could be solved for the Pt position in either space group, but yielded P positions only in $Pna2_1$.[10] Alternating least-squares cycles and difference maps eventually revealed the positions of all the remaining nonhydrogen atoms. The C_6H_5 rings of the anion were treated as rigid groups (C-C = 1.397 Å) in the least-squares refinement (on F_o). Scattering factors were taken from the usual tabulation and anomalous terms for the Pt and P atoms were included.[11] A correction was also made for decomposition (maximum 9.2%). The positions of all the hydrogen atoms could be discerned from a difference Fourier map after anisotropic refinement, and were included as fixed contributions to the F_c's after idealization (C-H = 1.00 Å, B's 1 Å^2 higher than those of the attached C atoms). The highest peaks in a final difference map were 0.6 e/Å^3 (about $\frac{1}{8}$ of a C peak) and no significant trends were observed in an analysis of $\Sigma w(|F_o| - |F_c|)^2$ [where $w = 4F_o^2/\sigma^2(F_o^2)$] as a function of $|F_o|$, sin θ/λ, and the Miller indices. The final parameters for the nongroup atoms are given in Table IIA; the derived positions of the ring carbon atoms and the rigid body parameters are listed in Table III. Tabulations of $10|F_o|$ vs. $10|F_c|$, principal root-mean-square amplitudes of vibration, and hydrogen-atom parameters are available.[12]

Crystal Structure of the PF_6^- Salt. Crystals of this salt[13] were also grown by slow evaporation of a CH_3OH/CH_2Cl_2 solution and were mounted in air. Details of this structure determination are given in Table I; the solution and refinement were straightforward and followed the outline given above. The maximum decomposition correction was 5.8%. All H-atom positions were located easily from difference maps and were included as fixed contributions. The methyl H's around C(6) appear to be disordered and two orientations were included with occupancy factors of 0.5. The highest peaks in a final difference map were 0.8 e/Å^3 (about $\frac{1}{10}$ of a C peak) and occur in the vicinity of the PF_6^- ion. An analysis of $\Sigma w(|F_o| - |F_c|)^2$ as a function of $|F_o|$, sin θ/λ, and Miller indices showed relatively poorer agreement at low θ values and high intensities. Attempts to refine an extinction parameter were unsuccessful, so this lack of agreement probably reflects the inability of the model to fully account for the large thermal motion (and/or disorder) of the PF_6^- ion. The final parameters are given in Table IIB. Listings of $10|F_o|$ vs. $10|F_c|$, principal root-mean-square amplitudes of vibration, and hydrogen-atom parameters are available.[12]

Spectra. Infrared spectra were recorded on a Perkin-Elmer 621 spectrophotometer as Nujol mulls or in CH_2Cl_2 or CH_3OH solutions and were calibrated with a polystyrene film. ^1H NMR spectra were obtained on a Varian CFT-20 spectrometer at 80 MHz with Me_4Si as an external standard.

Results

The infrared spectra between 1800 and 1600 cm^{-1} of the BPh_4^- and PF_6^- salts in CH_2Cl_2 solution and as Nujol mulls are shown in Figure 1. In CH_2Cl_2 the spectra of the ester carbonyl groups of the butenyl ligand are essentially the same for the two compounds. The absorptions at 1695 cm^{-1} are assigned to an uncoordinated ester carbonyl while the bands at 1574 and 1572 cm^{-1} of the BPh_4^- and PF_6^- salts are assigned to a coordinated C-O group. The frequency difference between the two sets of bands is attributed to the decrease in the bond order of the C-O bond upon coordination to the Pt. A number of examples of coordination of an ester carbonyl on the β carbon of an alkyl group have been reported and the absorption band of the coordinated C-O has usually been found between 1600 and 1500 cm^{-1}.[14-16] From these spectra structure III was assigned to the cation of both salts in solution.

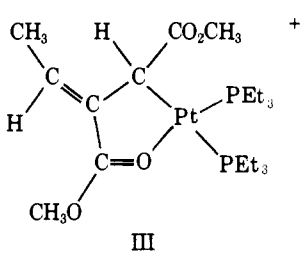

III

It is shown below that this structure is consistent with the NMR data.

The ^1H NMR spectra of the two salts in $CDCl_3$ solution are shown in Figure 2. The basic features of these two spectra are the same, although there are small differences in the chemical shifts. The observation of a pair of triplets for the methyl

Table II

A. Positional and Thermal Parameters for the Nongroup Atoms of $\{Pt[\eta^1\text{-}CH(COOCH_3)C(COOCH_3)=CHCH_3](PEt_3)_2\}BPh_4$

	x[a]	y	z	β_{11}[b]	β_{22}	β_{33}	β_{12}	β_{13}	β_{23}
Pt	0.093 31 (2)	0.118 10 (4)	0.25	12.9 (1)	84.6 (4)	77.9 (3)	−2.8 (2)	−0.5 (4)	1.5 (10)
P(1)	0.1294 (1)	0.0687 (3)	0.3973 (4)	15. (1)	95. (3)	99. (4)	−1. (1)	−5. (1)	20. (3)
P(2)	0.1578 (2)	0.1945 (4)	0.1666 (4)	16. (1)	108. (4)	102. (4)	−4. (2)	7. (1)	6. (3)
O(1)	0.0072 (5)	−0.0519 (10)	0.1368 (10)	30. (3)	132. (12)	98. (11)	−5. (5)	−14. (4)	−19. (10)
O(2)	0.0430 (4)	−0.1321 (8)	0.2726 (13)	31. (2)	84. (9)	108. (16)	−2. (3)	−3. (5)	5. (10)
O(3)	0.0513 (4)	0.1748 (9)	0.1226 (8)	17. (2)	122. (11)	82. (8)	−5. (4)	−3. (3)	14. (8)
O(4)	−0.0219 (4)	0.2266 (9)	0.0873 (9)	18. (2)	137. (12)	86. (9)	−1. (4)	−12. (4)	3. (8)
C(1)	0.0269 (5)	0.0517 (13)	0.2903 (11)	17. (2)	91. (13)	92. (16)	−5. (5)	−4. (4)	−9. (11)
C(2)	−0.0062 (5)	0.1377 (11)	0.2501 (25)	15. (2)	105. (14)	85. (11)	−2. (5)	2. (11)	−48. (22)
C(3)	−0.0431 (6)	0.1773 (13)	0.2983 (13)	16. (2)	126. (16)	99. (15)	0. (5)	−6. (5)	1. (12)
C(4)	−0.0611 (6)	0.1460 (16)	0.4033 (16)	20. (3)	174. (22)	126. (18)	14. (7)	10. (6)	8. (17)
C(5)	0.0225 (6)	−0.0458 (14)	0.2250 (16)	20. (3)	74. (14)	128. (28)	−6. (5)	10. (6)	1. (15)
C(6)	0.0443 (9)	−0.2326 (14)	0.2137 (13)	54. (7)	87. (16)	129. (23)	14. (8)	−1. (8)	−35. (13)
C(7)	0.0092 (7)	0.1795 (13)	0.1489 (14)	17. (3)	105. (15)	75. (14)	2. (6)	−9. (6)	−7. (12)
C(8)	−0.0043 (6)	0.2770 (18)	−0.0090 (14)	23. (3)	214. (25)	84. (14)	2.(7)	−19. (6)	32. (16)
C(11)	0.0958 (5)	−0.0182 (13)	0.4862 (13)	14. (2)	134. (16)	96. (13)	−6. (6)	4. (5)	21. (12)
C(12)	0.1238 (6)	−0.0606 (15)	0.5824 (13)	22. (3)	148. (17)	92. (14)	−6. (6)	−10. (6)	38. (14)
C(13)	0.1435 (6)	0.1826 (15)	0.4785 (12)	18. (3)	134. (18)	80. (13)	−14. (6)	−15. (5)	26. (13)
C(14)	0.1034 (9)	0.2591 (19)	0.4911 (18)	42. (6)	156. (23)	129. (21)	−17. (9)	−24. (10)	−29. (18)
C(15)	0.1835 (6)	−0.0055 (19)	0.3776 (22)	14. (3)	175. (24)	205. (28)	4. (8)	10. (8)	67. (24)
C(16)	0.1764 (8)	−0.1068 (18)	0.3199 (24)	34. (5)	154. (22)	263. (34)	39. (9)	35. (10)	52. (23)
C(21)	0.2048 (6)	0.2616 (19)	0.2320 (22)	20. (3)	304. (31)	214. (33)	−34. (8)	−17. (9)	164. (30)
C(22)	0.2418 (9)	0.3116 (26)	0.1562 (27)	38. (6)	357. (40)	314. (41)	−60. (14)	−31. (14)	210. (37)
C(23)	0.1389 (7)	0.2888 (22)	0.0724 (17)	16. (3)	231. (30)	132. (20)	−6. (8)	3. (7)	53. (21)
C(24)	0.1185 (9)	0.3861 (17)	0.1214 (25)	32. (5)	148. (23)	263. (35)	18. (9)	30. (11)	42. (25)
C(25)	0.1912 (12)	0.0957 (24)	0.0950 (33)	49. (8)	211. (37)	384. (57)	22. (14)	109. (19)	20. (37)
C(26)	0.1601 (14)	0.0140 (20)	0.0451 (29)	78. (11)	96. (23)	266. (41)	22. (13)	62. (19)	−29. (25)
B	0.3630 (5)	−0.0040 (12)	0.2537 (28)	12. (2)	106. (13)	110. (13)	−4. (4)	−9. (12)	−3. (31)

B. Positional and Thermal Parameters for the Nongroup Atoms of $\{Pt[\eta^3\text{-}CH_3CHC(CO_2CH_3)CHCO_2CH_3](PEt_3)_2\}PF_6$

	x[a]	y	z	β_{11}[b]	β_{22}	β_{33}	β_{12}	β_{13}	β_{23}
Pt	0.105 451 (18)	−0.228 189 (15)	−0.086 851 (8)	68.52 (19)	36.52 (11)	13.68 (4)	4.28 (14)	7.54 (6)	−0.12 (6)
P(1)	0.329 16 (14)	−0.260 36 (12)	−0.067 15 (7)	69.9 (13)	60.3 (10)	21.2 (3)	3.0 (9)	8.0 (5)	0.5 (5)
P(2)	0.034 80 (13)	−0.339 98 (10)	−0.167 32 (6)	76.5 (13)	40.5 (8)	16.6 (3)	5.4 (8)	8.7 (5)	−3.4 (4)
P(3)	0.411 29 (21)	0.115 25 (15)	0.285 70 (10)	137.3 (24)	65.4 (13)	30.9 (5)	0.9 (14)	1.5 (9)	0.1 (6)
F(1)	0.3806 (7)	0.1363 (5)	0.2125 (3)	384. (13)	149. (6)	42. (2)	51. (7)	47. (4)	31. (3)
F(2)	0.4092 (9)	0.2251 (4)	0.3032 (5)	382. (16)	88. (5)	97. (4)	25. (6)	−5. (6)	−13. (3)
F(3)	0.4234 (9)	0.0889 (6)	0.3571 (3)	484. (18)	209. (8)	35. (2)	87. (9)	−28. (4)	−10. (3)
F(4)	0.2584 (6)	0.1199 (7)	0.2817 (3)	167. (8)	303. (11)	71. (3)	−38. (8)	17. (4)	33. (5)
F(5)	0.4075 (11)	0.0049 (4)	0.2721 (3)	768. (24)	72. (4)	49. (2)	8. (8)	−28. (6)	−6. (2)
F(6)	0.5555 (7)	0.1153 (8)	0.2886 (5)	138. (8)	283. (12)	170. (6)	28. (8)	43. (6)	−10. (7)
O(1)	0.1203 (5)	−0.2170 (4)	0.0826 (2)	124. (6)	87. (4)	22. (1)	−24. (4)	2. (2)	10. (2)
O(2)	0.2726 (4)	−0.0985 (3)	0.0763 (2)	99. (5)	81. (3)	19. (1)	−22. (3)	5. (2)	−5. (1)
O(3)	−0.1447 (5)	−0.2981 (4)	−0.0140 (2)	157. (6)	70. (3)	28. (1)	−29. (4)	20. (2)	−5. (2)
O(4)	−0.1544 (4)	−0.1586 (3)	0.0441 (2)	136. (6)	77. (3)	23. (1)	1. (3)	30. (2)	−5. (2)
C(1)	0.1020 (6)	−0.1175 (4)	−0.0110 (2)	97. (6)	46. (3)	17. (1)	5. (4)	12. (2)	−3. (2)
C(2)	−0.0308 (5)	−0.1484 (4)	−0.0377 (2)	89. (6)	44. (3)	18. (1)	10. (3)	12. (2)	−3. (2)
C(3)	−0.0815 (6)	−0.1341 (4)	−0.1023 (2)	97. (6)	46. (3)	19. (1)	17. (4)	5. (2)	−5. (2)
C(4)	−0.0481 (7)	−0.0469 (5)	−0.1414 (3)	150. (9)	56. (4)	18. (1)	32. (5)	10. (3)	4. (2)
C(5)	0.1611 (6)	−0.1513 (5)	0.0536 (3)	91. (6)	59. (4)	17. (1)	−4. (4)	8. (2)	−4. (2)
C(6)	0.3424 (7)	−0.1280 (7)	0.1375 (3)	112. (8)	132. (7)	18. (1)	−16. (6)	−5. (3)	−4. (3)
C(7)	−0.1138 (6)	−0.2133 (5)	−0.0010 (3)	85. (6)	63. (5)	18. (1)	2. (4)	9. (2)	2. (2)
C(8)	−0.2252 (8)	−0.2146 (6)	0.0852 (4)	159. (10)	110. (7)	31. (2)	−14. (7)	39. (4)	−1. (3)
C(11)	0.4012 (6)	−0.3194 (6)	−0.1296 (3)	81. (6)	73. (5)	37. (2)	5. (5)	20. (3)	−12. (3)
C(12)	0.5520 (7)	−0.3308 (6)	−0.1172 (4)	81. (7)	93. (6)	46. (3)	6. (5)	21. (3)	−8. (3)
C(13)	0.4216 (7)	−0.1427 (6)	−0.0521 (4)	98. (7)	96. (6)	36. (2)	−27. (5)	19. (3)	−16. (3)
C(14)	0.3910 (10)	−0.0685 (7)	−0.1058 (5)	231. (15)	70. (6)	65. (4)	−46. (8)	56. (6)	−0. (4)
C(15)	0.3845 (7)	−0.3294 (7)	0.0055 (3)	117. (8)	101. (7)	28. (2)	27. (6)	2. (3)	14. (3)
C(16)	0.3166 (11)	−0.4292 (8)	0.0084 (5)	251. (17)	106. (8)	54. (3)	−26. (9)	−39. (6)	43. (4)
C(21)	0.1019 (6)	−0.3228 (5)	−0.2409 (2)	122. (7)	61. (4)	16. (1)	3. (4)	16. (2)	−4. (2)
C(22)	0.0980 (9)	−0.2151 (5)	−0.2628 (3)	225. (13)	67. (5)	21. (2)	−1. (6)	32. (4)	2. (2)
C(23)	−0.1450 (6)	−0.3366 (5)	−0.1926 (3)	92. (6)	55. (4)	24. (1)	3. (4)	6. (2)	−6. (2)
C(24)	−0.2047 (7)	−0.4174 (6)	−0.2405 (4)	100. (8)	92. (6)	36. (2)	−12. (5)	−4. (3)	−18. (3)
C(25)	0.0703 (6)	−0.4695 (4)	−0.1445 (3)	111. (7)	39. (3)	29. (2)	11. (4)	7. (3)	0. (2)
C(26)	−0.0075 (8)	−0.5049 (5)	−0.0935 (4)	197. (12)	55. (4)	34. (2)	1. (6)	20. (4)	13. (3)

[a] Estimated standard deviations in the least significant figure(s) are given in parentheses in this and all subsequent tables. [b] The form of the anisotropic thermal ellipsoid is $\exp[-(\beta_{11}h^2 + \beta_{22}k^2 + \beta_{33}l^2 + 2\beta_{12}hk + 2\beta_{13}hl + 2\beta_{23}kl)]$. The quantities given are the thermal coefficients $\times 10^4$.

Table III. Thermal Parameters and Derived Positional Parmeters for the Rigid Group Atoms of $\{Pt[\eta^1\text{-}CH(COOCH_3)C(COOCH_3)=CHCH_3](PEt_3)_2\}BPh_4$

atom	x	y	z	B, Å^2	atom	x	y	z	B, Å^2
R1C1	0.3506 (3)	−0.1358 (5)	0.2757 (8)	6.0 (3)	R3C1	0.4209 (3)	0.0162 (7)	0.2788 (8)	5.3 (3)
R1C2	0.3866 (3)	−0.2129 (7)	0.2757 (7)	6.0 (4)	R3C2	0.4353 (3)	0.0497 (8)	0.3785 (7)	6.8 (4)
R1C3	0.3755 (3)	−0.3226 (6)	0.2821 (7)	6.8 (4)	R3C3	0.4834 (4)	0.0601 (8)	0.4012 (7)	7.6 (4)
R1C4	0.3283 (4)	−0.3552 (6)	0.2885 (8)	8.8 (5)	R3C4	0.5170 (3)	0.0371 (8)	0.3242 (9)	8.3 (5)
R1C5	0.2923 (3)	−0.2782 (8)	0.2885 (8)	9.7 (6)	R3C5	0.5026 (3)	0.0036 (8)	0.2245 (8)	6.0 (4)
R1C6	0.3034 (3)	−0.1684 (7)	0.2822 (8)	7.3 (4)	R3C6	0.4546 (4)	−0.0068 (7)	0.2018 (6)	6.3 (4)
R2C1	0.3498 (4)	0.0273 (10)	0.1277 (7)	6.3 (4)	R4C1	0.3322 (4)	0.0747 (8)	0.3357 (8)	6.1 (4)
R2C2	0.3148 (4)	−0.0289 (8)	0.0732 (9)	7.1 (4)	R4C2	0.3294 (4)	0.1848 (8)	0.3124 (7)	6.4 (4)
R2C3	0.3042 (3)	−0.0012 (9)	−0.0304 (8)	7.2 (4)	R4C3	0.3084 (4)	0.2558 (6)	0.3837 (9)	7.2 (4)
R2C4	0.3286 (4)	0.0828 (9)	−0.0796 (7)	8.5 (5)	R4C4	0.2902 (4)	0.2167 (9)	0.4784 (9)	9.4 (5)
R2C5	0.3636 (4)	0.1390 (7)	−0.0250 (9)	8.6 (5)	R4C5	0.2931 (4)	0.1067 (9)	0.5017 (7)	9.2 (5)
R2C6	0.3742 (4)	0.1113 (9)	0.0786 (9)	7.6 (4)	R4C6	0.3141 (4)	0.0357 (6)	0.4304 (9)	7.0 (4)

Rigid Group Parameters

group	x_c[a]	y_c	z_c	δ[b]	ϵ	η
ring 1	0.3394 (3)	−0.2455 (6)	0.2821 (4)	1.341 (5)	−3.108 (6)	3.083 (6)
ring 2	0.3445 (3)	0.0412 (7)	0.0759 (6)	−0.770 (6)	−3.113 (6)	−1.902 (7)
ring 3	0.4690 (3)	0.0267 (4)	0.3015 (6)	−2.480 (16)	1.946 (6)	2.541 (16)
ring 4	0.3112 (2)	0.1457 (6)	0.4071 (6)	2.912 (8)	−2.471 (6)	0.979 (8)

[a] x_c, y_c, and z_c are the fractional coordinates of the origin of the rigid group. [b] The rigid group orientation angles δ, ϵ, and η (rad) are those defined previously (S. J. La Placa and J. A. Ibers, *Acta Crystallogr.*, **18**, 511 (1965)).

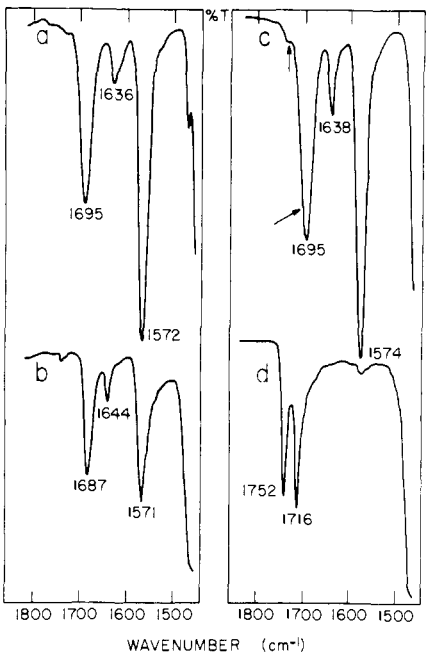

Figure 1. Solution and solid-state infrared spectra of the BPh_4^- and PF_6^- salts: (a) BPh_4^- salt in CH_2Cl_2 solution; (b) BPh_4^- salt as Nujol mull; (c) PF_6^- salt in CH_2Cl_2 solution; (d) PF_6^- salt as Nujol mull.

groups of the PEt_3 ligands is consistent with cis geometry at the platinum; a quintet would be anticipated if the phosphines were to adopt a trans geometry.[17,18] The single olefinic proton appears as a quartet, $J(H\text{-}CH_3) = 7$ Hz, at 6.50 and 6.70 ppm, respectively, for the BPh_4^- and PF_6^- salts; the aliphatic hydrogen on the α carbon appears at 3.24 and 3.36 ppm, respectively, as a doublet of doublets. Although large differences in the chemical shifts of the methyl esters are observed, these differences are expected. We have studied the NMR spectra of a large number of cationic complexes of this general type as both the BPh_4^- and PF_6^- salts. The difference in the chemical shifts of the two ester methyl groups is between 0.12 and 0.13 ppm for BPh_4^- salts and between 0.43 and 0.47 ppm for PF_6^- salts.

Although solution spectra of these two salts are very similar, their solid-state infrared spectra (Figure 1), obtained from Nujol mulls, differ dramatically. The BPh_4^- salt has absorption bands at 1687 and 1571 cm^{-1}, in good agreement with the solution spectrum, but the bands of the PF_6^- salt appear at 1752 and 1716 cm^{-1}. The latter spectrum suggests that the cation of the PF_6^- salt has two uncoordinated carbonyls in the solid state. Since crystallization conditions for the two salts were not identical it is important to consider the possibility of solvent effects. Crystals of both compounds were obtained by evaporation of CH_3OH/CH_2Cl_2 solutions, but the BPh_4^- salt crystallizes rapidly while the PF_6^- salt does not precipitate until most of the CH_2Cl_2 has evaporated. The infrared spectrum of the PF_6^- salt, however, is identical in the two solvents. The structural change observed for the PF_6^- salt is not then a solvent-dependent process but is a solution → solid state rearrangement. The interconversion is expected to be a low-energy process which would not include gross changes (e.g., cleavage or formation of C-H or C-C bonds) in the internal bonding of the organic ligand. Therefore we concluded that the η^1-allyl (structure III) to η^3-allyl (structure IV) rearrangement shown below had occurred for the cation of the PF_6^- salt upon crystallization.

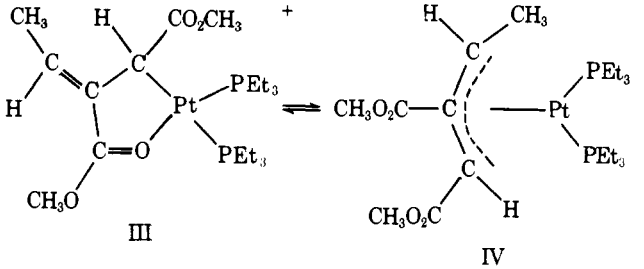

Since the structure of the PF_6^- salt is different in solution and in the solid state, some small fraction of the cation isolated in the solid state (structure IV) may exist in solution in equilibrium with the dominant form (structure III). All efforts to obtain a value for this equilibrium constant failed. We examined the NMR spectrum of the PF_6^- salt in a variety of solvents ranging from good coordinating solvents such as CH_3CN and Me_2SO to noncoordinating solvents such as 1,2-dichloroethane and CH_2Cl_2 over the temperature range −100 to +100 °C and found no detectable changes in the spectra.

The infrared spectrum of the PF_6^- salt in CH_2Cl_2 does have two small shoulders at approximately 1750 and 1715 cm^{-1} (see

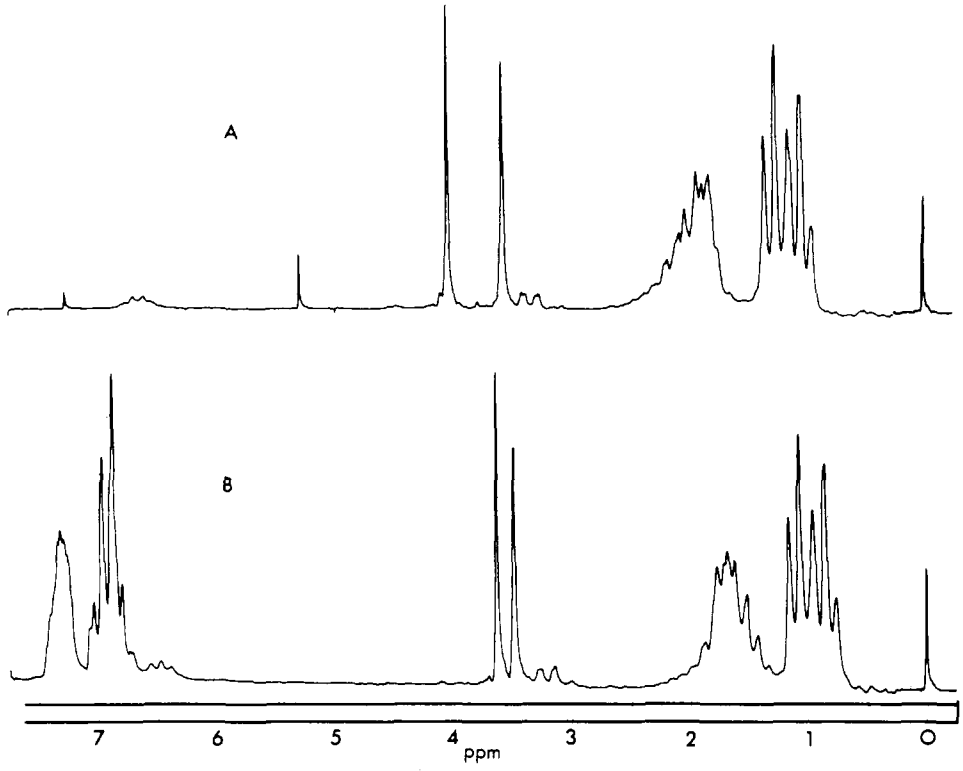

Figure 2. ^1H NMR spectra in $CDCl_3$: (A) PF_6^- salt; (B) BPh_4^- salt. The singlet at 5.32 ppm in (A) is CH_2Cl_2.

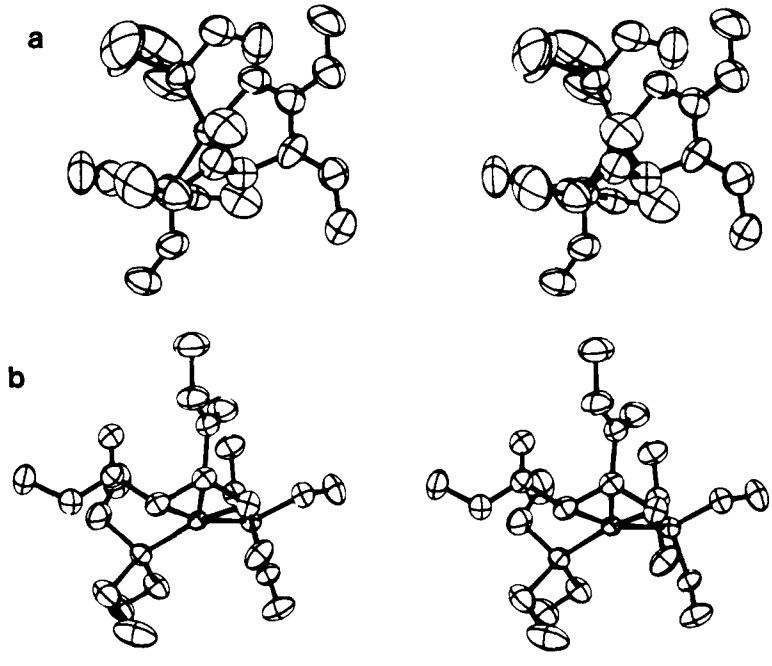

Figure 3. (a) A stereoscopic drawing of the $\{Pt[\eta^1\text{-}CH(COOCH_3)C(COOCH_3)=CHCH_3](PEt_3)_2\}^+$ cation. The orientation of the organic ligand is the same in this and the following drawing. The origins and scales of the two drawings are also identical so that the sizes of the thermal ellipsoids may be compared. In this and the following drawings the shapes of the atoms correspond to 50% probability contours of thermal motion and H atoms have been omitted for the sake of clarity. (b) A stereoscopic drawing of the $\{Pt[\eta^3\text{-}CH_3CHC(CO_2CH_3)CHCO_2CH_3](PEt_3)_2\}^+$ cation.

arrows in Figure 1) which could be attributed to the structure IV. However, caution must be exercised in making such assignments and these peaks may have no significance. If these shoulders can be attributed to η^3-allyl cations, then a comparison of the intensities of the two types of carbonyl bands indicates that the equilibrium between the two structures strongly favors the η^1-allyl structure III.

Description of the Structures. The crystal structure determinations for these two salts confirm the structural and stereochemical assignments. More importantly, the structures demonstrate the absence of any special short interactions between ions; in both salts all interionic distances are longer than the sums of the van der Waals radii of the atoms involved. Stereoviews of the two cations are shown in Figure 3. The differences in the sizes of the thermal ellipsoids are notable; the thermal motion of the cation in the BPh_4^- salt is significantly greater than in the PF_6^- salt. The BPh_4^- salt is also considerably less dense (1.37 vs. 1.73 g cm^{-3}) than the PF_6^- salt, again suggesting that the crystal packing is tighter in the latter compound. The stereoviews also show that, while the η^1

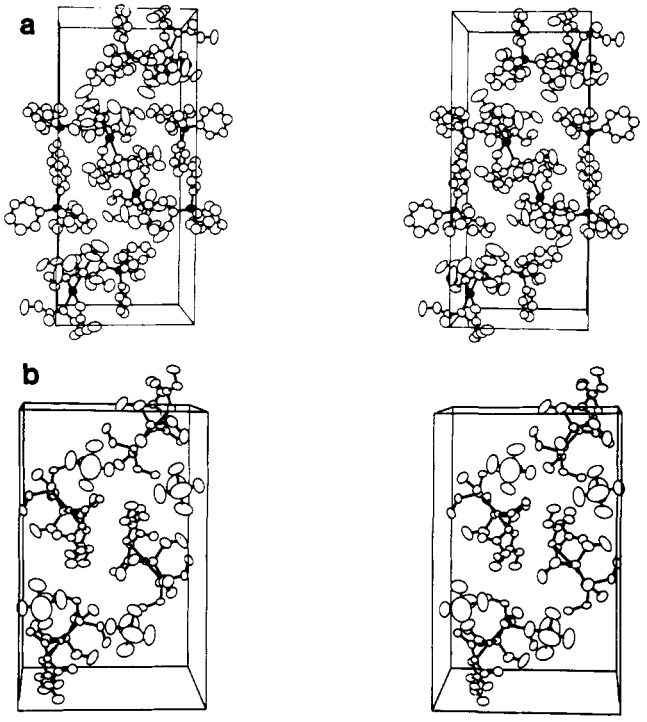

Figure 4. (a) A stereoscopic drawing of the contents of a unit cell of $\{Pt[\eta^1\text{-}CH(COOCH_3)C(COOCH_3)=CHCH_3](PEt_3)_2\}BPh_4$. Two additional BPh_4^- ions have been included and the B and Pt atoms darkened to clarify the packing. The a axis runs vertically upward, the b axis runs from left to right, and the c axis points into the paper. (b) A stereoscopic drawing of the contents of a unit cell of $\{Pt[\eta^3\text{-}CH_3CHC(CO_2CH_3)\text{-}CHCO_2CH_3](PEt_3)_2\}PF_6$. The b axis runs from left to right, the a axis points out of the paper, and the c axis runs vertically upward.

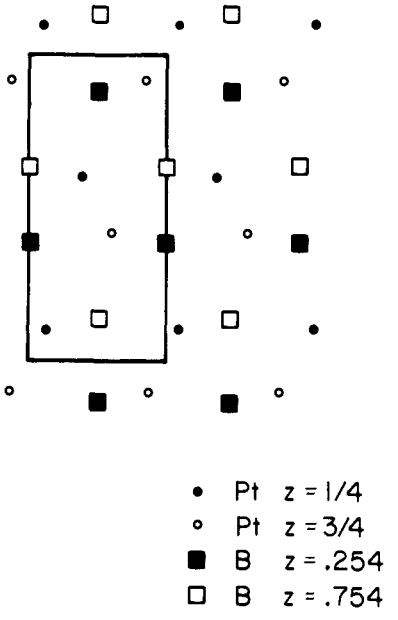

Figure 5. A diagram of the locations of the Pt and B atoms in the BPh_4^- salt. The axes in this projection are in the same orientation as in Figure 4a.

cation is roughly spherical, the η^3 cation has a rather "flat" region as a result of the near planarity of the organic ligand. In the PF_6^- salt pairs of these regions are related across an inversion center, the planes being separated by about 3.8 Å.

The differences in crystal packing between the two salts are illustrated in Figures 4-6. The globular anions in the BPh_4^- salt can be viewed as forming a distorted hexagonal-close-packed lattice through which run columns of cations which are

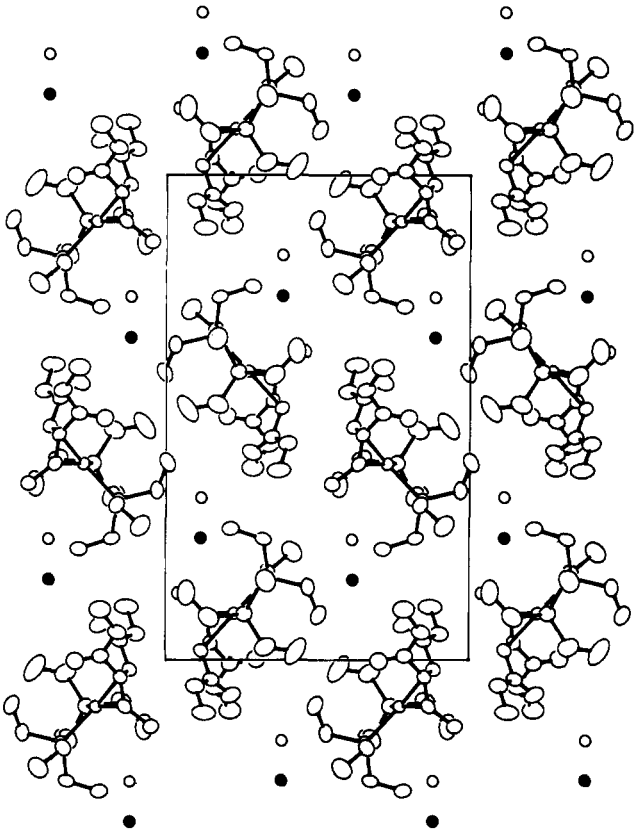

Figure 6. A projection of the structure of the PF_6^- salt showing a cation layer and the positions of the neighboring PF_6^- ions. The axes are in the same orientation as in Figure 4b. The dark circles indicate anions above the plane of the paper, and the open circles, anions behind the plane. Since $\beta \neq 90°$ translation-equivalent anions are offset in the vertical direction.

parallel to c. The relatively high thermal motion in this structure suggests that the packing is rather loose, and it is probably dominated by van der Waals interactions. The PF_6^- salt, on the other hand, can be seen as being composed of layers of cations perpendicular to a^*. Within each layer the cation pairs described above form rows parallel to b, alternate rows being tipped in opposite senses with respect to c to give a herringbone arrangement. The PF_6^- anions also form rows parallel to b which separate both the cation rows and layers. Consequently each pair of cations is surrounded by an approximate square-prismatic arrangement of anions. These crystals are relatively hard, and it is likely that ionic interactions (i.e., Madelung considerations) are important in this structure.

The organic ligands and inner coordination spheres of the two cations are displayed in Figure 7. A selection of distances, angles and least-squares planes for the two cations is given in Figure 7 and Table IV; information about the dimensions of the anions is listed in Table V. Unfortunately, the much larger standard deviations in the BPh_4^- structure, a result of the greater thermal motion in this salt, preclude detailed comparisons of some of the bond lengths and angles. The most noteworthy feature of the η^1 cation is the strong trans influence of the sp^3-hybridized C(1) as compared to the carbonyl oxygen O(3). The difference of 0.090 (6) Å between the two Pt-P bond lengths is one of the largest such differences seen within a Pt(II) complex.[19] The three sections of the organic ligand which are expected to be planar (i.e., [C(1), C(2), C(3), C(4), C(7)], [C(1), C(5), O(1), O(2)], and [C(2), C(7), O(3), O(4)]) are so to within experimental error, and all bond lengths are close to expected values. The last of these three planar segments is twisted relative to the first about the C(2)-C(7) bond so that the dihedral angle between them is 25.2°. The

Table IV. Selected Distances, Angles, and Least-Squares Planes for the Two Structure Determinations

	BPh_4^- salt	PF_6^- salt
	Bond Angles (deg)	
P(1)-Pt-C(1)	95.6 (4)	97.7 (2)
P(1)-Pt-O(3)	172.0 (3)	
P(1)-Pt-C(3)		157.0 (2)
P(2)-Pt-C(1)	166.2 (4)	161.1 (2)
P(2)-Pt-O(3)	87.4 (3)	
P(2)-Pt-C(3)		96.0 (1)
C(1)-Pt-C(3)		67.2 (2)
C(2)-C(1)-Pt	101.3 (10)	69.4 (3)
C(2)-C(3)-Pt		67.8 (3)
C(2)-C(1)-C(5)	109.6 (15)	119.2 (5)
Pt-C(1)-C(5)	104.9 (11)	115.3 (4)
C(1)-C(2)-C(3)	127.0 (25)	120.9 (5)
C(1)-C(2)-C(7)	111.4 (16)	122.0 (5)
C(3)-C(2)-C(7)	121.5 (19)	116.3 (5)
C(2)-C(3)-C(4)	126.9 (20)	124.9 (5)
C(4)-C(3)-Pt		104.2 (4)
C(1)-C(5)-O(1)	127.4 (18)	126.1 (5)
C(1)-C(5)-O(2)	111.0 (17)	110.9 (5)
O(1)-C(5)-O(2)	121.3 (18)	123.0 (5)
C(2)-C(7)-O(3)	120.7 (16)	124.7 (5)
C(2)-C(7)-O(4)	119.0 (6)	109.3 (5)
O(3)-C(7)-O(4)	120.2 (17)	125.9 (5)
C(5)-O(2)-C(6)	117.1 (16)	116.0 (5)
C(7)-O(3)-Pt	110.2 (11)	
C(7)-O(4)-C(8)	117.5 (14)	114.1 (5)
	Conformation Angles (deg)	
C(1)-C(2)-C(3)-C(4)	0.5 (28)	34.0 (8)
O(1)-C(5)-C(1)-C(2)	20.8 (26)	14.7 (9)
O(3)-C(7)-C(2)-C(1)	25.0 (22)	111.5 (7)
	Displacements from Planes (Å)	
	(i) Plane Defined by Pt, P(1), P(2)	
C(1)	−0.103 (17)	0.138 (6)
C(2)	0.838 (17)	0.371 (6)
C(3)	1.754 (19)	−0.605 (6)
O(3)	0.221 (12)	
C(7)	0.672 (18)	
	(ii) Plane Defined by C(1), C(2), C(3)	
C(4)	0.011 (58)	−0.691 (16)
C(5)	1.267 (24)	0.268 (11)
C(7)	−0.080 (59)	0.242 (19)
	Dihedral Angle (deg)	
Pt, P(1), P(2) / C(1), C(2), C(3)	48.2 (6)	112.5 (5)

Table V. Dimensions of the Anions

	BPh_4^-	PF_6^-
bond lengths, Å		
av	1.688 (11)	1.528 (2)
range	1.674 (2)-1.693 (17)	1.460 (7)-1.566 (5)
bond angles, deg		
av	109.4 (6)	89.5 (1) (cis)
		175.3 (3) (trans)
range	107.5 (16)-111.1 (16)	85.1 (4)-93.9 (5) (cis)
		172.7 (5)-177.6 (5) (trans)

coordination plane itself is significantly distorted as can be seen from the displacements given in Table IV.

The most interesting feature of the η^3 cation is the asymmetry in the bonding of the Pt to the allyl group; the Pt is 0.060 (7) Å closer to C(1) than to C(3). However, the difference in the two C-C bonds within the allyl, 0.035 (12) Å, is not really significant. Another aspect of the bonding asymmetry is the twist of the allyl moiety with respect to the P(1)-Pt-P(2) plane which can be seen in Figures 3b and 7b and is also revealed in

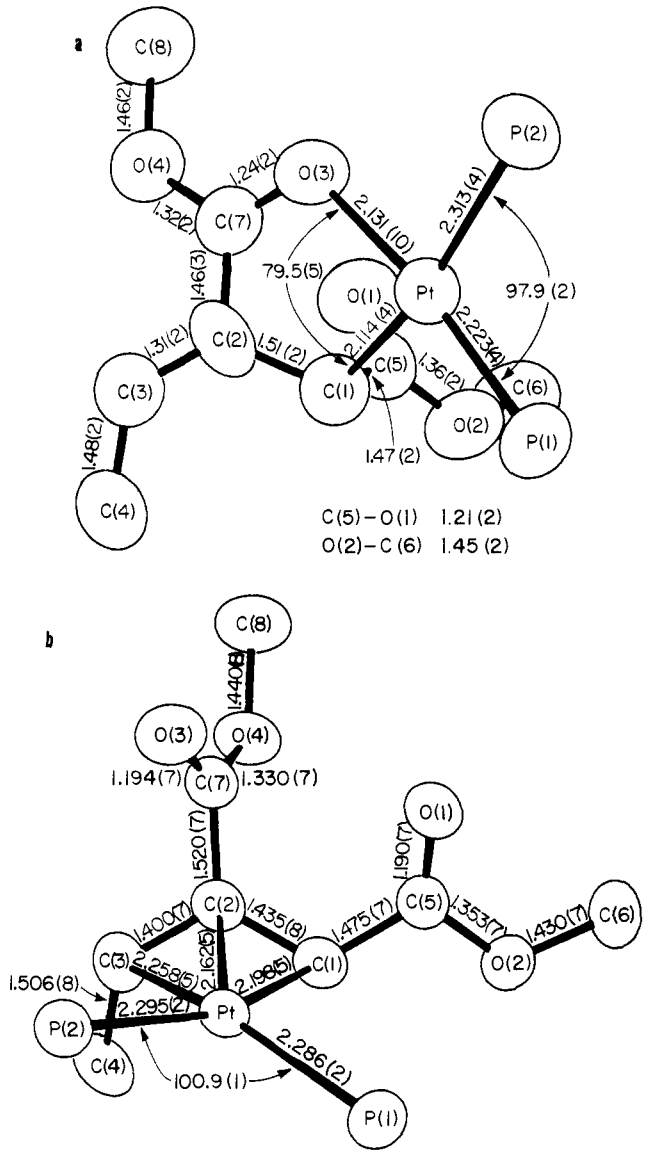

Figure 7. (a) The organic ligand and inner coordination sphere of the $\{Pt[\eta^1\text{-}CH(COOCH_3)C(COOCH_3)=CHCH_3](PEt_3)_2\}^+$ cation. In this and the following drawing the cations have been rotated 180° about a vertical axis relative to their orientations in Figure 3. (b) The organic ligand and inner coordination sphere of the $\{Pt[\eta^3\text{-}CH_3CHC(CO_2CH_3)\text{-}CHCO_2CH_3](PEt_3)_2\}^+$ cation.

the displacements of C(1), C(2), and C(3) from the P(1)-Pt-P(2) plane (Table IV). These distortions from idealized coordination geometry most likely result from the presence of different substituents on C(1) and C(3) and are probably influenced by both steric and electronic considerations. Finally, mixing of σ and π orbitals in the allyl is demonstrated by the displacements of C(4), C(5), and C(7) from the plane of C(1), C(2), and C(3) (see Table IV). The especially large deviation of C(4) (which unlike the other two is displaced away from the metal) is also reflected in the C(4)-C(3)-C(2)-C(1) conformation angle of 34.0 (8)°.

Discussion

In this system the crystal lattice of the PF_6^- salt clearly stabilizes a form of the cation which is not present in solution in appreciable concentration. Therefore it must be concluded that the interactions between ions in the η^3-allyl PF_6^- salt are sufficiently more favorable than they would be for a η^1-allyl PF_6^- salt that the intraionic energy difference is overcome. While it is not unusual for the long-range, directional forces

present in crystals to stabilize molecular species which are not dominant in some other phase, essentially all such examples have involved conformational distortions in which bonds are not altered, or changes in bond lengths or angles which are relatively small. In this system, however, there are large differences in the bonding patterns between the solution and solid-state structures.

Greater solid densities are usually associated with more negative, i.e., more favorable, lattice energies. Therefore the denser packing of the PF_6^- relative to the BPh_4^- salt is probably related to the stabilization of the η^3-allyl cation by the former. Although no especially short contacts are present in either structure, the PF_6^- salt has an appreciably higher density and considerably less thermal motion than does the BPh_4^- salt. The melting points of the two compounds are the same (124–125 °C), although there is a ca. 20% difference in their formula weights.

It is not a simple matter to determine the origin of the dense packing in the PF_6^- salt, especially since both van der Waals and ionic interactions are involved. When doing lattice energy calculations based on the atom-atom potential method in complicated structures it is observed[20] that hundreds of intermolecular interactions contribute rather similar amounts of energy to the lattice sum. It may therefore be very misleading to single out a small number of such interactions and view them as structure determining. In spite of this caveat it appears that the interaction of the "flat" regions of η^3-allyl cations across centers of symmetry may contribute to the efficient packing in the PF_6^- salt. Although no interatomic contact across the inversion center is smaller than the sum of the van der Waals radii of the atoms concerned, the number of relatively short nonbonded contacts per atom is quite large.

The difference in the anions is presumably also important in determining the crystal packing. While both anions are roughly spherical, the BPh_4^- ion has an irregular surface which allows some interpenetration of the cation and anion. The sizes of the two anions are very different; the BPh_4^- ion, which is approximately the same size as the Pt-allyl cation, occupies about five times the volume required by a PF_6^- ion. The greater localization of charge in the PF_6^- salt may contribute to a more favorable Madelung energy than can be obtained in the BPh_4^- salt. Thinking that anion size (i.e. charge-to-volume ratio) might be the determining factor in the crystal packing we made repeated attempts to produce solids with BF_4^- and ClO_4^- as counterions, but had no success. These two ions have charge distributions with T_d rather than O_h symmetry and their volumes are 20–30% smaller than the volume of PF_6^-; apparently these differences are large enough to preclude crystallization.

The observation of two different forms of the platinum-allyl cation in compounds differing only in the identity of a noncoordinating anion is strong evidence that the η^1- and η^3-allyl structures are similar in energy and are connected by a low-energy pathway. While it does not appear to be possible to measure the equilibrium constant for the process, it is possible to give an estimate for the upper bound to the energy difference. Calculations in several laboratories of the lattice energy stabilization of nonequilibrium conformations in molecular crystals have given ca. 5 kcal/mol as the upper bound for such lattice effects.[20,21] While this estimate may not be strictly applicable to a system which includes ionic interactions, the sizes of the ions in this system are large enough that the crystals are more molecular than ionic in nature. Such an energy value is also consistent with the absence in solution of identifiable infrared bands arising from the η^3-allyl cation. Ratios of 20:1, 100:1, and 1000:1 for the two species correspond to free-energy differences at 300 K of 1.8, 2.7, and 4.1 kcal/mol, respectively.

Acknowledgment. Purchase of the X-ray diffractometer used in this study was supported by an NSF Departmental Equipment Grant (CHE 77-07445).

Supplementary Material Available: Principal root-mean-square amplitudes of vibration, calculated hydrogen positional parameters, and observed and calculated structure factor amplitudes (56 pages). Ordering information is given on any current masthead page.

References and Notes

(1) Pearson, R. G.; Laurent, M. *Isr. J. Chem.* **1977**, *15*, 243–246.
(2) Volger, H. C.; Vrieze, K. *J. Organomet. Chem.* **1967**, *9*, 527–536.
(3) Kaduk, J. A.; Ibers, J. A. *J. Organomet. Chem.* **1977**, *139*, 199–207.
(4) Vrieze, K.; Volger, H. C. *J. Organomet. Chem.* **1967**, *9*, 537–548. Clark, H. C.; Kurosawa, H. *Inorg. Chem.* **1973**, *12*, 357–362.
(5) Kurosawa, H.; Yoshida, G. *J. Organomet. Chem.* **1976**, *120*, 297–311.
(6) Attig, T. G. *J. Organomet. Chem.* **1978**, *145*, C13–C17.
(7) Attig, T. G. *Inorg. Chem.* **1978**, *17*, 3097–3102.
(8) Burmeister, J. L.; Gysling, H. J.; Lim, J. C. *J. Am. Chem. Soc.* **1969**, *91*, 44–47.
(9) Melpolder, J. B.; Burmeister, J. L. *Inorg. Chim. Acta* **1975**, *15*, 91–104.
(10) In addition to various local programs for the IBM 370/165 computer, local versions of the following programs were employed: Zalkin's FORDAP Fourier program, the Busing–Levy ORFFE error function program, the absorption correction program AGNOST, and Johnson's thermal ellipsoid plotting program ORTEP. Our version of Ibers' least-squares program NUCLS, which in its nongroup form closely resembles the Busing–Levy ORFLS program, was also used.
(11) Cromer, D. T.; Waber, J. T. "International Tables for X-ray Crystallography", Vol. IV; Kynoch Press: Birmingham, England.
(12) See paragraph at end of paper regarding supplementary material.
(13) Attig, T. G.; Sasser, R. L., unpublished results.
(14) Blackmore, T.; Bruce, M. I.; Stone, F. G. A. *J. Chem. Soc., Dalton Trans.* **1974**, 106–112.
(15) Harbourne, D. A.; Stone, F. G. A. *J. Chem. Soc. A* **1968**, 1765–1771.
(16) Bannister, W. D.; Booth, B. L.; Haszeldine, R. N.; Loader, P. L. *J. Chem. Soc. A* **1971**, 930–934.
(17) Randall, E. W.; Shaw, D. *Mol. Phys.* **1965**, *10*, 41–48.
(18) Clark, H. C.; Dixon, K. R.; Jacobs, W. J. *J. Am. Chem. Soc.* **1968**, *90*, 2259–2266.
(19) Appleton, T. G.; Clark, H. C.; Manzer, L. E. *Coord. Chem. Rev.* **1973**, *10*, 335–422.
(20) Brock, C. P. *Acta Crystallogr., Sect. A* **1977**, *33*, 898–902.
(21) Bernstein, J.; Hagler, A. T. *J. Am. Chem. Soc.* **1978**, *100*, 673–681.